Glabridin attenuates LTA-induced alveolar macrophage migration via activation of the Nrf2/HO-1 pathway

CHIH-HSUAN HSIA[1-3*], CHUN-MING YANG[1,4-6*], CHAO-CHIEN CHANG[1,7,8], TING-LIN YEN[9,10], ARIEF GUNAWAN DARMANTO[1,11], CHI-CHANG HUANG[3] and JOEN-RONG SHEU[1]

[1]Graduate Institute of Medical Sciences, College of Medicine, Taipei Medical University, Taipei 110, Taiwan, R.O.C.; [2]Translational Medicine Center, Shin Kong Wu Ho-Su Memorial Hospital, Taipei 111, Taiwan, R.O.C.; [3]Graduate Institute of Sports Science, National Taiwan Sport University, Taoyuan City 333325, Taiwan, R.O.C.; [4]Department of Neurology, Chi Mei Medical Center, Tainan 710, Taiwan, R.O.C.; [5]School of Medicine, College of Medicine, National Sun Yat-sen University, Kaohsiung 80424, Taiwan, R.O.C.; [6]School of Medicine, Chung Shan Medical University, Taichung 40201, Taiwan, R.O.C.; [7]Department of Cardiovascular Center, Cathay General Hospital, Taipei 106, Taiwan, R.O.C.; [8]School of Medicine, College of Medicine, Fu Jen Catholic University, New Taipei City 242, Taiwan, R.O.C.; [9]Department of Medical Research, Cathay General Hospital, Taipei 106, Taiwan, R.O.C.; [10]Department of Pharmacology, School of Medicine, College of Medicine, Taipei Medical University, Taipei 110, Taiwan, R.O.C.; [11]School of Medicine, Universitas Ciputra, Surabaya 60219, Indonesia

Received July 6, 2025; Accepted October 28, 2025

DOI: 10.3892/mmr.2025.13758

Abstract. Oxidative stress and macrophage migration contribute to chronic inflammation and resultant tissue damage. The nuclear factor erythroid 2-related factor 2 (Nrf2) antioxidant pathway plays a key role in maintaining redox balance and modulating immune cell behavior. Lipoteichoic acid (LTA), a component of Gram-positive bacterial membranes, activates macrophages and overproduces reactive oxygen species (ROS), causing oxidative stress and aberrant macrophage migration. In the present study, the effects of glabridin (GBD), a flavonoid from licorice with antioxidant potential, on LTA-mediated oxidative stress and alveolar macrophage migration were investigated. GBD pretreatment reduced intracellular ROS levels, as measured through 2',7'-dichlorofluorescin diacetate and dihydroethidium staining. Immunofluorescence microscopy revealed increased nuclear translocation of Nrf2 following GBD treatment. Western blotting demonstrated elevated expression of Nrf2 and its downstream target, heme oxygenase-1 (HO-1). Cotreatment with the Nrf2 inhibitor ML385 attenuated GBD-mediated Nrf2 activation and HO-1 expression, suggesting involvement of the Nrf2/HO-1 pathway. Functionally, GBD inhibited LTA-induced macrophage migration, and this effect was attenuated by ML385 cotreatment. These findings demonstrate that GBD suppresses LTA-induced macrophage migration, at least in part, through the Nrf2/HO-1 signaling pathway, suggesting potential therapeutic relevance in inflammatory lung diseases.

Correspondence to: Dr Joen-Rong Sheu, Graduate Institute of Medical Sciences, College of Medicine, Taipei Medical University, 250 Wuxing Street, Xinyi, Taipei 110, Taiwan, R.O.C.
E-mail: sheujr@tmu.edu.tw

*Contributed equally

Key words: glabridin, nuclear factor erythroid 2-related factor 2/heme oxygenase-1 pathway, macrophage migration, lipoteichoic acid, alveolar macrophages

Introduction

Gram-positive bacteria are a major class of pathogens that trigger the host's innate immune response, predominantly through their surface component lipoteichoic acid (LTA), a potent immunostimulatory agent (1-3). Alveolar macrophages are the resident immune cells in the alveolar space, where they serve as the first line of defense against inhaled pathogens and as key drivers of pulmonary immune responses (4). LTA activates alveolar macrophages through its interaction with Toll-like receptor 2 (TLR2), producing inflammatory cytokines and reactive oxygen species (ROS). Although both mediators play a role in the host's defensive response to infection, they can also contribute to lung tissue injury (5,6). Given their central role in lung immune surveillance, alveolar macrophages are uniquely vulnerable to redox perturbations induced by microbial insults (7). Prolonged oxidative stress disrupts redox balance and amplifies inflammatory signaling, causing cellular dysfunction and damaging pulmonary tissue (8). Given that alveolar macrophages can be both sources and targets of oxidative stress, careful regulation of redox balance is required to sustain pulmonary homeostasis during infection (7,9).

Cells combat oxidative injury through endogenous antioxidant systems, which are predominantly mediated through the nuclear factor erythroid 2-related factor 2 (Nrf2) pathway (10-12). When Nrf2 is activated in response to oxidative signals, it dissociates from its cytoplasmic repressor, Keap1 and translocates to the nucleus, where it induces

transcription of antioxidant and cytoprotective genes such as heme oxygenase-1 (HO-1) (12,13). Studies have demonstrated that the Nrf2/HO-1 axis contributes to numerous oxidative injury models and it may have protective effects against inflammatory lung diseases (14,15). Although LTA induced macrophage activation is well established, the extent to which Nrf2/HO-1 signaling contributes in alveolar macrophages remains unclear. Additionally, whether pharmacological agents or naturally derived products can induce protective effectors through this redox-sensitive pathway under LTA-induced stress is unknown (16).

Glabridin (GBD; Fig. 1A), a prenylated isoflavan derived from *Glycyrrhiza glabra* (licorice root), has been reported to exhibit antioxidant and anti-inflammatory properties in variouS cellular models (17). These properties take effect in part through the activation of Nrf2-dependent pathways (18). However, whether GBD can mitigate LTA-induced oxidative stress in alveolar macrophages and restore redox balance through Nrf2/HO-1 signaling remains to be elucidated. Moreover, the potential influence of this pathway on macrophage migration under inflammatory conditions has not been studied. The present study therefore investigated the protective effects of GBD on LTA-induced oxidative stress and macrophage migration, focusing on the potential involvement of Nrf2/HO-1 signaling.

Materials and methods

Reagents and materials. GBD (≥98%; cat. no. 11843) and dihydroethidium (DHE; cat. no. 12013) were purchased from Cayman Chemical Company. LTA (cat. no. L2515), dimethyl sulfoxide (DMSO; cat. no. D8418), bovine serum albumin (BSA; cat. no. A5611), 2',7'-dichlorofluorescin diacetate (DCFDA; cat. no. D6883), phenylmethylsulfonyl fluoride (PMSF; cat. no. P7626), sodium orthovanadate (cat. no. S6508), sodium pyrophosphate (cat. no. S6422), aprotinin (cat. no. A1153), leupeptin (cat. no. L2884), sodium fluoride (NaF; cat. no. 201154), and paraformaldehyde (PFA; cat. no. P6148) were purchased from MilliporeSigma. Anti-Nrf2 (cat. no. GTX103322) polyclonal antibodies (pAb) were purchased from GeneTex, Inc. Anti-HO-1 (cat. no. 10701-1-AP) pAb and β-actin (cat. no. 60008-1-Ig) monoclonal antibodies were purchased from Proteintech Group, Inc. Hybond-P polyvinylidene difluoride (PVDF) membranes (cat. no. GE10600023) and enhanced chemiluminescence Western blotting detection reagent (cat. no. GERPN2232) were obtained from Cytiva. Horseradish peroxidase (HRP)-conjugated donkey anti-rabbit immunoglobulin G (IgG; cat. no. AP182P), and sheep anti-mouse IgG (cat. no. SAB3701093) were obtained from MilliporeSigma. GBD was dissolved in DMSO, stored at 4˚C, and diluted to the working concentration in cell culture medium before use. DMSO (0.1%) served as the vehicle control for all experiments.

Cell culture. MH-S cells, a murine alveolar macrophage cell line, were obtained from ATCC (cat. no. CRL-2019) and cultured in RPMI-1640 medium (cat. no. A1049101; Gibco; Thermo Fisher Scientific, Inc.) supplemented with 10% fetal bovine serum (FBS; cat. no. 26140079; Gibco; Thermo Fisher Scientific, Inc.) and 1% penicillin-streptomycin. Cells were maintained at 37˚C in a 5% CO_2 humidified atmosphere. Cells were used for experiments between passages 4 and 8. The cell line was confirmed to be free of mycoplasma contamination using a Mycoplasma Detection Kit (cat. no. rep-mys-10; InvivoGen).

Cell viability assay. The MH-S cells were seeded in 24-well culture plates at a density of $1x10^5$ cells per well and cultured in RPMI-1640 medium containing 10% FBS for 24 h. Once the cells reached the required confluence, they were treated with varying concentrations of GBD (10-40 μM) or 0.1% DMSO for 30 min and then subjected to LTA stimulation (10 μg/ml) for 24 h at 37˚C. An MTT assay (cat. no. AM0815-0005; Bionovas Biotechnology Co., Ltd.) was performed to assesS cell viability, with results expressed as a percentage calculated using the following formula:

$$\text{Cell Survival Rate } (\%) = \frac{\text{ODsample} - \text{ODblank}}{\text{ODDMSO} - \text{ODblank}} x100\%$$

Measurement of intracellular ROS. Intracellular ROS production was assessed with DCFDA and DHE. Cells were cultured on coverslips in 6-well plates at a density of $5x10^4$ cells/well and treated with 0.1% DMSO or 20 μM GBD. The cells then underwent LTA stimulation for 30 min followed by incubation with DCFDA (10 μM) or DHE (5 μM) for 30 min at 37˚C in the dark. The cells were washed twice with phosphate-buffered saline (PBS), and the coverslips were mounted onto glass slides with Fluoroshield medium containing DAPI (cat. no. ab104139; Abcam). A DM6 CS confocal microscope (Leica Microsystems GmbH) with a x63 oil immersion objective was used for immediate fluorescence signal visualization. Fluorescence intensity was quantified using ImageJ software, version 1.54g (NIH).

Immunofluorescence staining assay. Cells were cultured on coverslips at a density of $5x10^4$ per well and pretreated with 0.1% DMSO, 20 μM GBD, or 5 μM ML385 (cat. no. 21114; Cayman Chemical Company) for 30 min. The cells were subsequently stimulated with LTA for 3 or 6 h and fixed after treatment in 4% PFA for 10 min at room temperature. The fixed cells were permeabilized with 0.1% Triton X-100, followed by blocking in 5% BSA for 30 min. The prepared cells were incubated with target-specific primary antibodies (1:100) overnight at 4˚C. After thorough PBS washing, the specimens were exposed to Alexa Fluor 488-conjugated goat anti-rabbit IgG secondary antibody (1:2,000; cat. no. ab150077; Abcam) for 1 h at room temperature. Following three additional PBS washes, the coverslips were mounted onto glass slides with Fluoroshield medium containing DAPI.

Cell imaging was performed with the aforementioned confocal microscope system. ImageJ software was used to analyze fluorescence intensity. For Nrf2 nuclear translocation, nuclear regions of interest (ROIs) were identified through DAPI staining. For HO-1 analysis, ROIs were selected around individual cells to calculate the mean fluorescence intensity (MFI) of the whole cell was calculated after background subtraction.

Cell transfection. Cells were seeded in 6-well plates at a density of $2x10^5$ cells/well and cultured until 80% confluence. Cells were then transfected with either a small interfering

(si)RNA targeting Nrf2 [*Nfe2l2* siRNA: 5'-AGCAUUUUA ACAUGUUAACAG-3' (sense) and 5'-GUUAACAUGUUA AAAUGCUAU-3' (antisense)] or a negative control siRNA [si-Ctrl: 5'-UUCUCCGAACGUGUCACGUTT-3' (sense) and reverse 5'- ACGUGACACGUUCGGAGAATT-3' (antisense); cat. no. HY-RS09246; MedChemExpress], using a transfection reagent (cat. no. HY-K2017, MedChemExpress) and 50 nM siRNA diluted in serum-free medium, according to the manufacturer's instructions. Following 6 h incubation at 37˚C, the transfection mixture was replaced with complete medium, and cells were further cultured for 24 h before subsequent treatments. Knockdown efficiency was verified by reverse transcription-quantitative (RT-q) PCR.

RT-qPCR. Total RNA was extracted from MH-S cells ($5x10^6$ cells) with a NucleoSpin RNA Kit (cat. no. 740955.50; Macherey-Nagel) according to the manufacturer's instructions. RNA purity and concentration were assessed with a NanoDrop spectrophotometer (Thermo Fisher Scientific, Inc.). Complementary DNA was synthesized from 2 μg total RNA with the SuperScript IV First-Strand Synthesis System (cat. no. 18091050; Thermo Fisher Scientific, Inc.). RT-qPCR was performed with Fast SYBR Green Master Mix (cat. no. 4385612; Applied Biosystems; Thermo Fisher Scientific, Inc.). Amplification was performed with a StepOnePlus Real-Time PCR System (Applied Biosystems; Thermo Fisher Scientific, Inc.) with an initial hot-start activation at 95˚C for 1 min, followed by 45 cycles of denaturation at 95˚C for 5 sec and annealing/extension at 60˚C for 1 min. The following primers were used: Nrf2, forward 5'-AGCAGGACATGGAGCAAGTT-3' and reverse 5'-TTCTTTTTCCAGCGAGGAGA-3'; HO-1, forward 5'-GCACTATGTAAAGCGTCTCC-3' and reverse 5'-GACTCTGGTCTTTGTGTTCC-3'; and GAPDH, forward 5'-GAACATCATCCCTGCATCCA-3' and reverse 5'-GCCAGT GAGCTTCCCGTTCA-3'. GAPDH was used as the internal control. The primer sequences used for IL-1β, TNF-α, IL-6 and SOD1 are listed in Table SI. Relative gene expression levels were calculated according to the $2^{-\Delta\Delta Cq}$ method (19). All experiments were independently repeated ≥4 times.

Determination of nitric oxide and malondialdehyde levels. The detailed procedures for the determination of nitric oxide (NO) and malondialdehyde (MDA) levels are described in the Supplementary Methods.

Western blot analysis. MH-S cells ($8x10^5$ per ml) were cultured and preincubated with DMSO, GBD, or ML385 for 30 min at 37˚C. Cells underwent LTA stimulation or were left untreated for 3 or 6 h. The cells were lysed in lysis buffer containing aprotinin (10 μg/ml), PMSF (1 mM), leupeptin (2 μg/ml), NaF (10 mM), sodium orthovanadate (1 mM), and sodium pyrophosphate (5 mM) for 1 h at 4˚C. Subsequently, the samples were centrifuged at 13,500 x g for 30 min, and protein concentration was determined through a Bradford protein assay (cat. no. 5000006; Bio-Rad Laboratories, Inc.). Equal amounts of total protein (50 μg) were separated through 10% SDS-PAGE and then transferred onto polyvinylidene difluoride membranes (MilliporeSigma). Membranes were blocked in 5% BSA in Tris-buffered saline with 0.1% Tween-20 (TBST) at room temperature for 1 h and incubated with primary antibodies (anti-Nrf2, cat. no. GTX103322, GeneTex; anti-HO-1, cat. no. 10701-1-AP and anti-β-actin, cat. no. 60008-1-Ig, Proteintech) diluted 1:1,000 in TBST overnight at 4˚C. The membranes were then washed and incubated with HRP-conjugated secondary antibodies (donkey anti-rabbit IgG, cat. no. AP182P; and sheep anti-mouse IgG, cat. no. SAB3701093, MilliporeSigma) diluted 1:5,000 in TBST for 1 h at room temperature. Protein bands were quantified with a video densitometer and BioProfil BioLight software (v2000.01; Vilber Lourmat).

Wound healing assay. Cell migration was assessed through a wound healing assay performed in 24-well plates. A sterile 20-μl pipette tip was used to create a scratch in the confluent cell monolayer. Cells were incubated in serum-free medium with or without treatment. Images were captured at 0, 6, and 24 h after the scratch was created. Wound width was analyzed with ImageJ software, version 1.54g (NIH). The wound closure percentage was calculated according to the following formula:

$$\text{Wound closure}(\%) = \frac{[\text{Wound width (0 h)} - \text{Wound width (6 h or 24 h)}]}{\text{Wound width (0 h)}} \text{x}100\%$$

Transwell migration assay. Cell migration was assessed using Transwell inserts with 8 μm pore size (SPL Life Sciences, FL, USA) in 24-well plates. MH-S cells ($1x10^5$) were resuspended in medium containing 2% FBS and seeded into the upper chamber in 200 μl medium. The lower chambers were also filled with 600 μl of medium containing 2% FBS, and the plates were incubated at 37˚*C* for 30-60 min to allow cell attachment. Cells in the upper chamber were then treated with DMSO, GBD, or ML385 for 30 min in medium containing 2% FBS at 37˚*C*. After treatment, the medium in the lower chambers was replaced with fresh medium containing 2% FBS, with or without LTA (10 μg/ml), to serve as the chemoattractant.

After 6 or 24 h of incubation at 37˚C in a humidified 5% CO_2 incubator, non-migrated cells on the upper surface of the membrane were gently removed with cotton swabs. Cells that migrated to the lower surface were fixed with 4% PFA for 15 min at room temperature, washed twice with PBS, and stained with 0.2% crystal violet for 3 min at room temperature. Excess stain was removed by washing twice with PBS. Migrated cells were imaged and counted under an inverted microscope at x100 magnification. Relative migration was calculated as the ratio of the number of migrated cells in each treatment group to that in the DMSO group, which was defined as 1.

Statistical analysis. At least four independent replicates were performed for all experiments. Data are expressed as means±standard deviation (SD). Significance was determined through one-way analysis of variance followed by a Student-Newman-Keuls post hoc test. For datasets containing >3 groups, Tukey's post hoc test was used. $P<0.05$ was considered to indicate a statistically significant difference.

Results

GBD attenuates LTA-induced oxidative stress in MH-S cells. An MTT assay was performed to assess GBD cytotoxicity in MH-S cells. MH-S cells were treated with 10, 20 and 40 μM

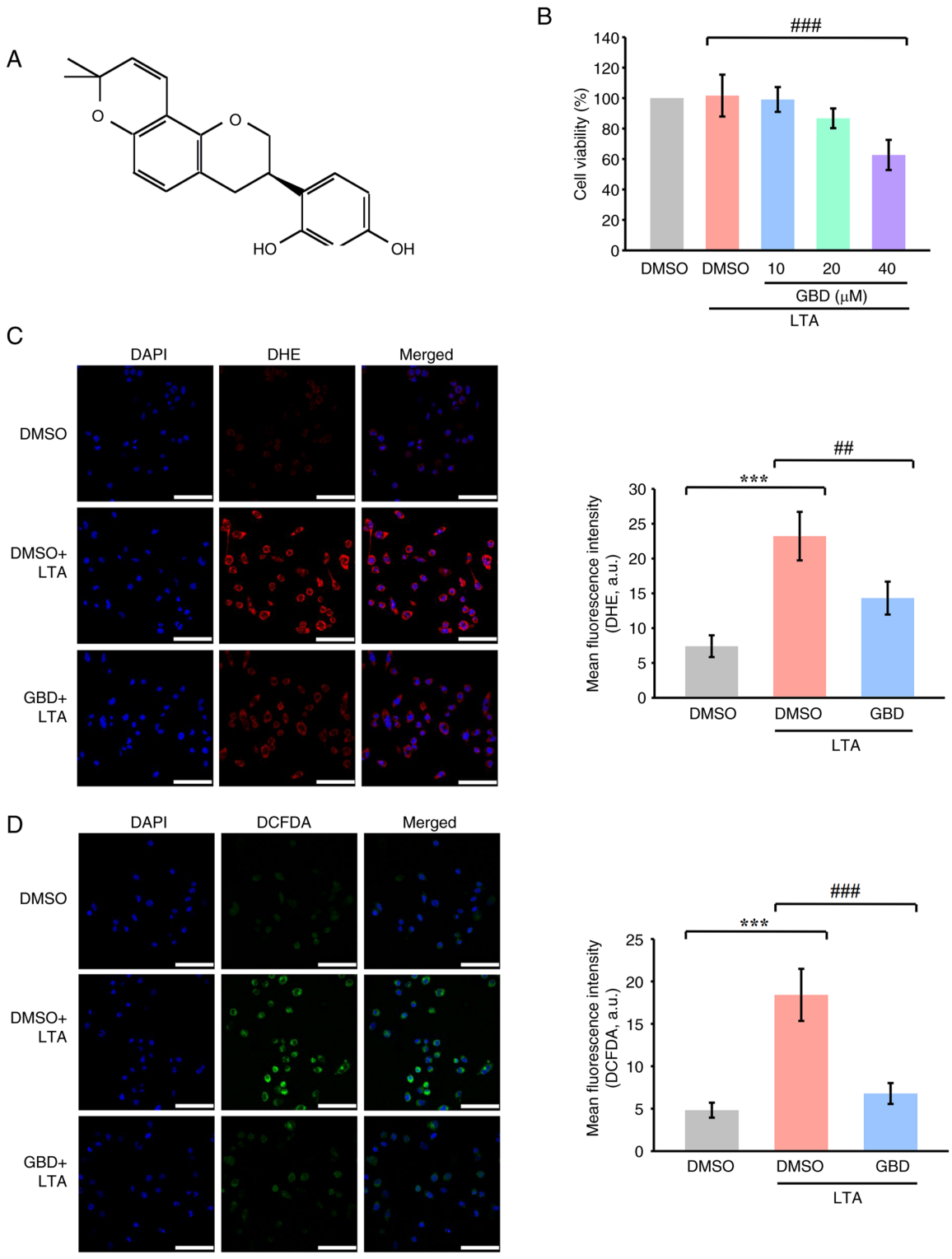

Figure 1. GBD reduces LTA-induced ROS production in MH-S cells. (A) Chemical structure of GBD. (B) MTT assay of cell viability. Cells were pretreated with various concentrations of GBD (10, 20 and 40 μM) or 0.1% DMSO for 30 min and then stimulated with LTA (10 μg/ml) for 24 h. (C) Representative fluorescence images and quantification of DHE staining in MH-S cells. (D) Representative fluorescence images and quantification of DCFDA staining. Cells were pretreated with GBD (20 μM) for 1 h and then stimulated with LTA (10 μg/ml) for 30 min. Experimental groups for C and D: CTRL, DMSO+LTA, and GBD+LTA. Scale bar, 50 μm. Data are presented as means±SD (n=4). ***P<0.001 vs. DMSO; $^{\#\#}$P<0.01, and $^{\#\#\#}$P<0.001 vs. DMSO+LTA. GBD glabridin; LTA, lipoteichoic acid; ROS, reactive oxygen species; DMSO, dimethyl sulfoxide; DHE, dihydroethidium staining; DCFDA. 2',7'-dichlorofluorescin diacetate.

of GBD in the presence of LTA (10 μg/ml) for 24 h. Whereas 40 μM of GBD reduced cell viability below 80%, 10 and 20 μM had no significant cytotoxic effects (Fig. 1B). To determine the effective concentration, cells were treated with 0, 5, 10, 20, and 30 μM GBD for 24 h. Increasing concentrations of GBD reduced proliferation, with an IC_{50} of ~18 μM (Fig. S1). Based on both of these findings, 20 μM was selected as the working concentration for subsequent experiments.

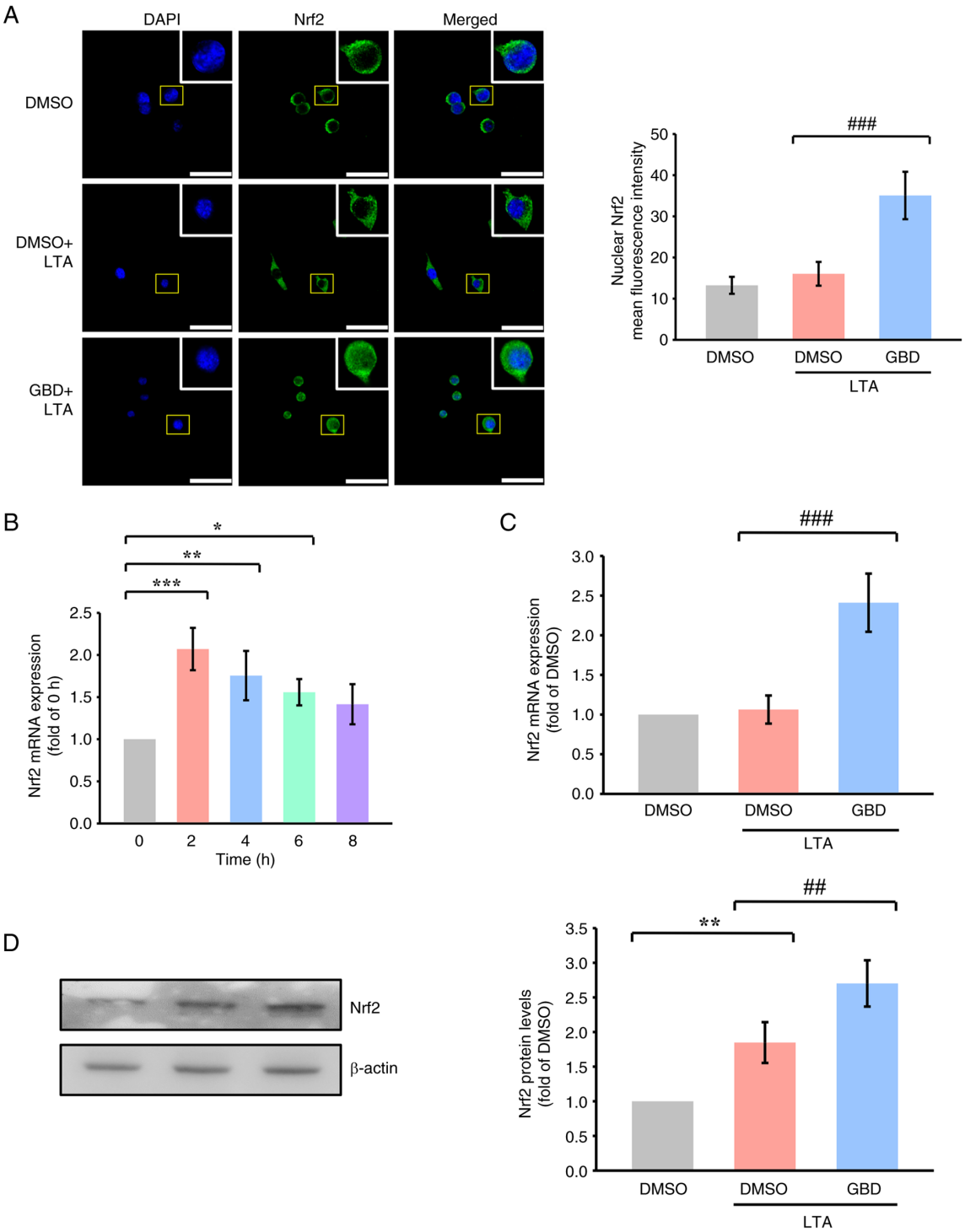

Figure 2. GBD activates Nrf2 signaling in response to LTA. MH-S cells were pretreated with GBD for 30 min and then stimulated with LTA. (A) Confocal images indicating Nrf2 nuclear translocation 3 h poststimulation. Scale bar, 50 μm. (B) Time-course of Nrf2 mRNA expression after LTA stimulation (0, 2, 4, 6, and 8 h). (C) Nrf2 mRNA expression was determined through reverse transcription-quantitative PCR 2 h poststimulation, as described in the materials and methods section. (D) Western blot analysis of Nrf2 protein levels 3 h after LTA stimulation. Data are presented as means±SD. *P<0.05, **P<0.01 and ***P<0.001 vs. 0 h or DMSO; $^{\#\#}$P<0.01 and $^{\#\#\#}$P<0.001 vs. DMSO+LTA. GBD glabridin; Nrf2, nuclear factor erythroid 2-related factor 2; LTA, lipoteichoic acid; DMSO, dimethyl sulfoxide.

LTA stimulation markedly increased intracellular ROS production, as indicated by elevated fluorescence in both DCFDA and DHE staining (Fig. 1C and D), which suggests the oxidative environment in the MH-S cells was enhanced. Pretreatment with 20 μM GBD markedly suppressed LTA-induced ROS accumulation. Quantitative analysis revealed markedly reduced fluorescence intensity in GBD-treated cells compared with the LTA group, as measured by DHE and DCFDA staining, indicating that GBD effectively mitigated LTA-induced oxidative stress.

GBD activates Nrf2 signaling in LTA-stimulated MH-S cells. The present study investigated whether Nrf2 signaling contributed to the antioxidative effects of GBD. Confocal microscopy

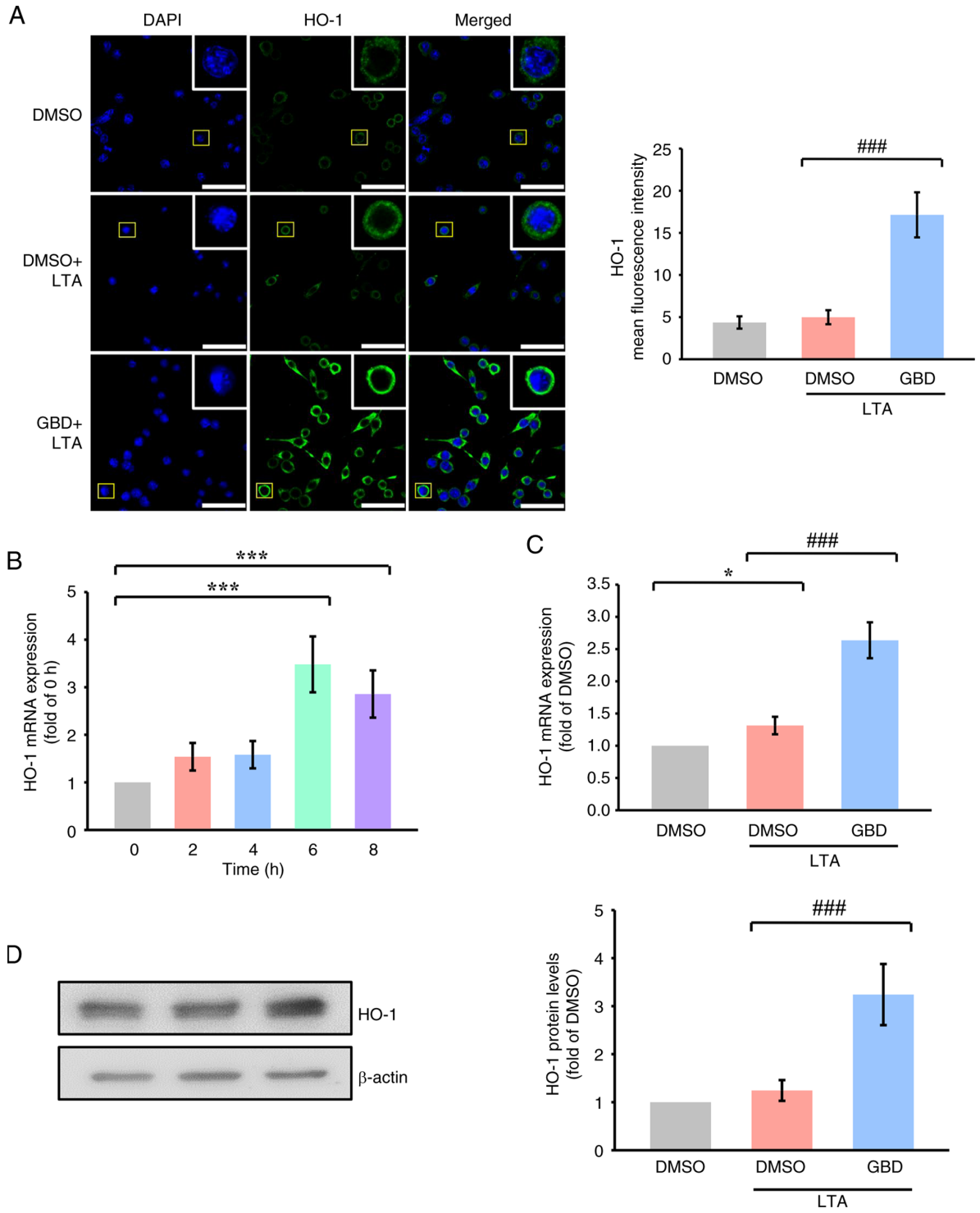

Figure 3. GBD increases HO-1 expression through Nrf2 signaling under LTA challenge. MH-S cells were pretreated with GBD for 30 min and then stimulated with LTA. (A) Confocal images of HO-1 expression 6 h poststimulation. Scale bar, 50 μm. (B) Time-course of HO-1 mRNA expression after LTA stimulation (0, 2, 4, 6, and 8 h). (C) HO-1 mRNA expression was determined by reverse transcription-quantitative PCR. (D) HO-1 protein expression analyzed through western blotting 6 h poststimulation. Data are presented as means±SD (n=4). *P<0.05 and ***P<0.001 vs. 0 h or DMSO; $^{\#\#\#}$P<0.001 vs. DMSO+LTA. GBD glabridin; HO-1, heme oxygenase-1; Nrf2, nuclear factor erythroid 2-related factor 2; LTA, lipoteichoic acid; DMSO, dimethyl sulfoxide.

revealed that LTA stimulation alone resulted in minimal Nrf2 nuclear localization, whereas GBD pretreatment markedly increased Nrf2 nuclear accumulation (Fig. 2A).

Time-course analysis indicated that Nrf2 mRNA peaked 2 h after LTA stimulation (Fig. 2B); thus, 2 h was selected as the representative time point for mRNA analysis. Nrf2 mRNA levels were markedly elevated in the GBD+LTA group compared with in the DMSO+LTA group (Fig. 2C). Western blot analysis performed at 3 h post-LTA stimulation showed that Nrf2 protein levels were increased following GBD treatment (Fig. 2D).

GBD upregulates HO-1 expression following Nrf2 activation. HO-1 expression was further examined as a downstream target of Nrf2. Confocal imaging revealed that GBD increased HO-1

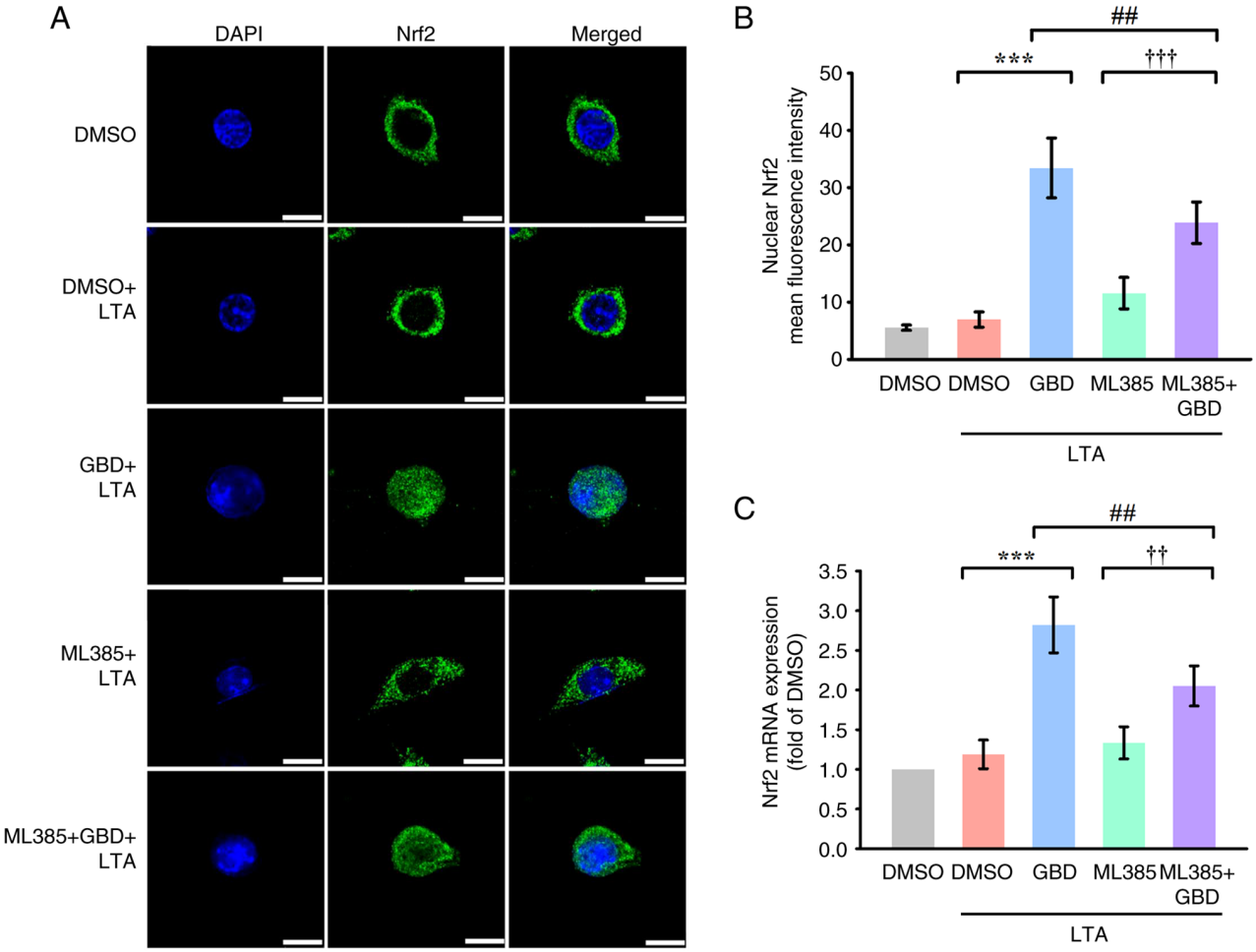

Figure 4. ML385 inhibits GBD-induced Nrf2 activation in LTA-stimulated MH-S cells. MH-S cells were pretreated with DMSO (0.1%), GBD (20 μM), or ML385 (5 μM) for 30 min and then stimulated with LTA. (A) Confocal microscopy of Nrf2 nuclear localization 3 h poststimulation. Scale bar, 10 μm. (B) Quantification of Nrf2 nuclear accumulation based on nuclear mean fluorescence intensity. (C) Nrf2 mRNA expression 2 h poststimulation, analyzed through reverse transcription-quantitative PCR. Data are presented as means ± SD. ***P<0.001 vs. DMSO+LTA; $^{\#\#}$P<0.01 vs. GBD+LTA; ††P<0.01 and †††P<0.001 vs. ML385+LTA. GBD glabridin; Nrf2, nuclear factor erythroid 2-related factor 2; LTA, lipoteichoic acid; DMSO, dimethyl sulfoxide.

fluorescence intensity 6 h after LTA stimulation relative to LTA treatment alone (Fig. 3A). Time-course analysis revealed that HO-1 mRNA expression peaked 6 h following LTA stimulation (Fig. 3B); thus, 6 h was selected as the representative time point for subsequent analysis. GBD also markedly upregulated HO-1 mRNA and protein levels 6 h after treatment (Fig. 3C and D), confirming its downstream activation of Nrf2. HO-1 is a cytoprotective enzyme with antioxidant properties. Its upregulation by GBD may represent one mechanism through Nrf2 activation contributes to redox homeostasis. These results align with the observed decrease in ROS accumulation and support the role of HO-1 as a key effector in GBD-mediated regulation of oxidative stress.

ML385 attenuates GBD-induced activation of Nrf2 and HO-1. The selective inhibitor ML385 (5 μM) was used to investigate the Nrf2-dependence of GBD-induced activation of Nrf2 and HO-1. Confocal microscopy indicated that ML385 markedly reduced the nuclear accumulation of Nrf2 in GBD-treated cells at 3 h (Fig. 4A and B). Additionally, RT-qPCR analysis revealed that ML385 suppressed GBD-induced expression of Nrf2 mRNA (Fig. 4C), indicating transcriptional inhibition.

ML385 attenuated HO-1 fluorescence intensity at 6 h, as confirmed through confocal imaging (Fig. 5A and B), and markedly decreased HO-1 mRNA levels in GBD-treated cells (Fig. 5C). These findings suggested that GBD-mediated upregulation of the Nrf2/HO-1 pathway is substantially dependent on Nrf2 activity, given that pharmacological inhibition of Nrf2 impaired both nuclear localization and downstream gene expression.

Genetic inhibition of Nrf2 reduces GBD-induced HO-1 expression. To further validate the role of Nrf2 in mediating GBD's effects, the present study performed siRNA knockdown experiments. Transfection with siRNA targeting Nrf2 (siNrf2) markedly reduced Nrf2 mRNA expression under basal conditions compared with a negative control siRNA (si-Ctrl; Fig. S2). Furthermore, Nrf2 knockdown markedly attenuated the GBD-induced upregulation of HO-1 mRNA (Fig. 5D and E). These results, together with the pharmacological inhibition by ML385, supported the involvement of Nrf2 in GBD-mediated HO-1 induction.

In addition to the Nrf2/HO-1 pathway, GBD also influenced inflammatory and oxidative stress-related factors in

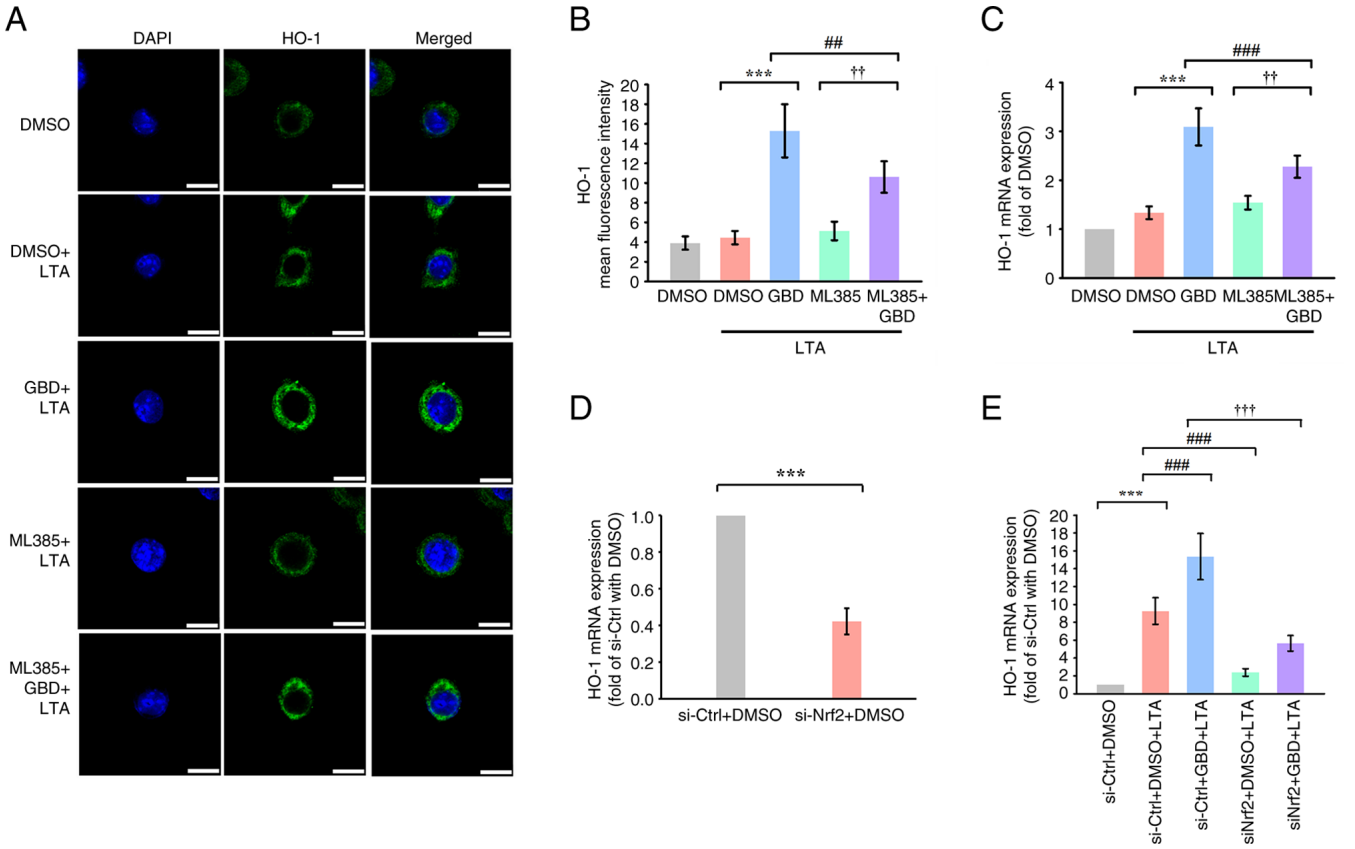

Figure 5. Pharmacological and genetic inhibition of Nrf2 attenuates GBD-induced HO-1 expression. MH-S cells were pretreated with the indicated compounds for 30 min and then stimulated with LTA. (A) Immunofluorescence analysis of HO-1 expression 6 h poststimulation. Scale bar, 10 μm. (B) Immunofluorescence image evaluation of HO-1 mean fluorescence intensity. (C) HO-1 mRNA expression 6 h poststimulation, determined through RT-qPCR. (D and E) Effect of Nrf2 knockdown on GBD-induced HO-1 expression. MH-S cells were transfected with control siRNA (siNC) or Nrf2 siRNA (siNrf2) for 6 h, followed by the indicated treatments. HO-1 mRNA levels were measured by RT-qPCR. Data are presented as means ± SD. ***P<0.001 vs. DMSO+LTA (B-C) or si-Ctrl+DMSO (D and E); $^{\#\#}$P<0.01 and $^{\#\#\#}$P<0.001 vs. GBD+LTA (B-C) or si-Ctrl+DMSO+LTA (E); ††P<0.01 and †††P<0.001 vs. ML385+LTA (B-C) or si-Ctrl+GBD+LTA (E). Nrf2, nuclear factor erythroid 2-related factor 2; GBD, glabridin; LTA, lipoteichoic acid; HO-1, heme oxygenase-1; RT-qPCR, reverse transcription-quantitative PCR; si, short interfering; DMSO, dimethyl sulfoxide.

LTA-stimulated MH-S cells. GBD significantly decreased the mRNA expression of IL-1β, TNF-α and IL-6, while the expression of SOD1 remained unchanged at 6 h (Fig. S3). Furthermore, GBD reduced MDA and NO levels at 24 h. These findings provide additional evidence supporting the antioxidative and anti-inflammatory potential of GBD.

Nrf2 contributes to the inhibitory effect of GBD on LTA-induced macrophage migration. Wound healing assays revealed that LTA markedly promoted MH-S cell migration at 6 and 24 h. GBD pretreatment suppressed this effect at both time points (Fig. 6A and B). Notably, cotreatment with Nrf2 inhibitor ML385 attenuated the antimigratory effects of GBD, as evidenced by markedly higher closure in the ML385+GBD+LTA group than in the GBD+LTA group at 6 and 24 h. In addition, migration in ML385+GBD+LTA group remained lower than in ML385+LTA group at 6 h, although this difference was not sustained at 24 h. These findings suggested that activation of the Nrf2/HO-1 axis at least partially mediates the inhibitory effects of GBD.

To further validate the antimigratory effects of GBD, Transwell assays were performed to assess directional cell migration. LTA stimulation markedly enhanced macrophage migration at both 6 and 24 h compared with the DMSO group (Fig. 6D). GBD pretreatment markedly attenuated this increase. Consistent with Nrf2 involvement, ML385 treatment in combination with LTA promoted migration, and importantly, cotreatment with ML385 partially reversed the inhibitory effect of GBD. These results corroborated the wound-healing findings and indicated that the antimigratory effects of GBD were mediated, at least in part, by Nrf2.

Discussion

Regulation of macrophage migration has gained increasing attention in inflammatory contexts, given that the aberrant migratory behavior of activated macrophages contributes to tissue damage and disease progression (20). Control over immune cell movement could limit excessive inflammatory responses and promote resolution (21). Although several studies have demonstrated the involvement of oxidative and inflammatory signaling in macrophage motility (22,23), the specific modulatory role of natural compounds remains uncertain. The findings of the present study suggested that GBD suppresses macrophage migration following LTA stimulation and that this effect was associated with the activation of the Nrf2/HO-1 pathway (Fig. 7). Thus, GBD may be a

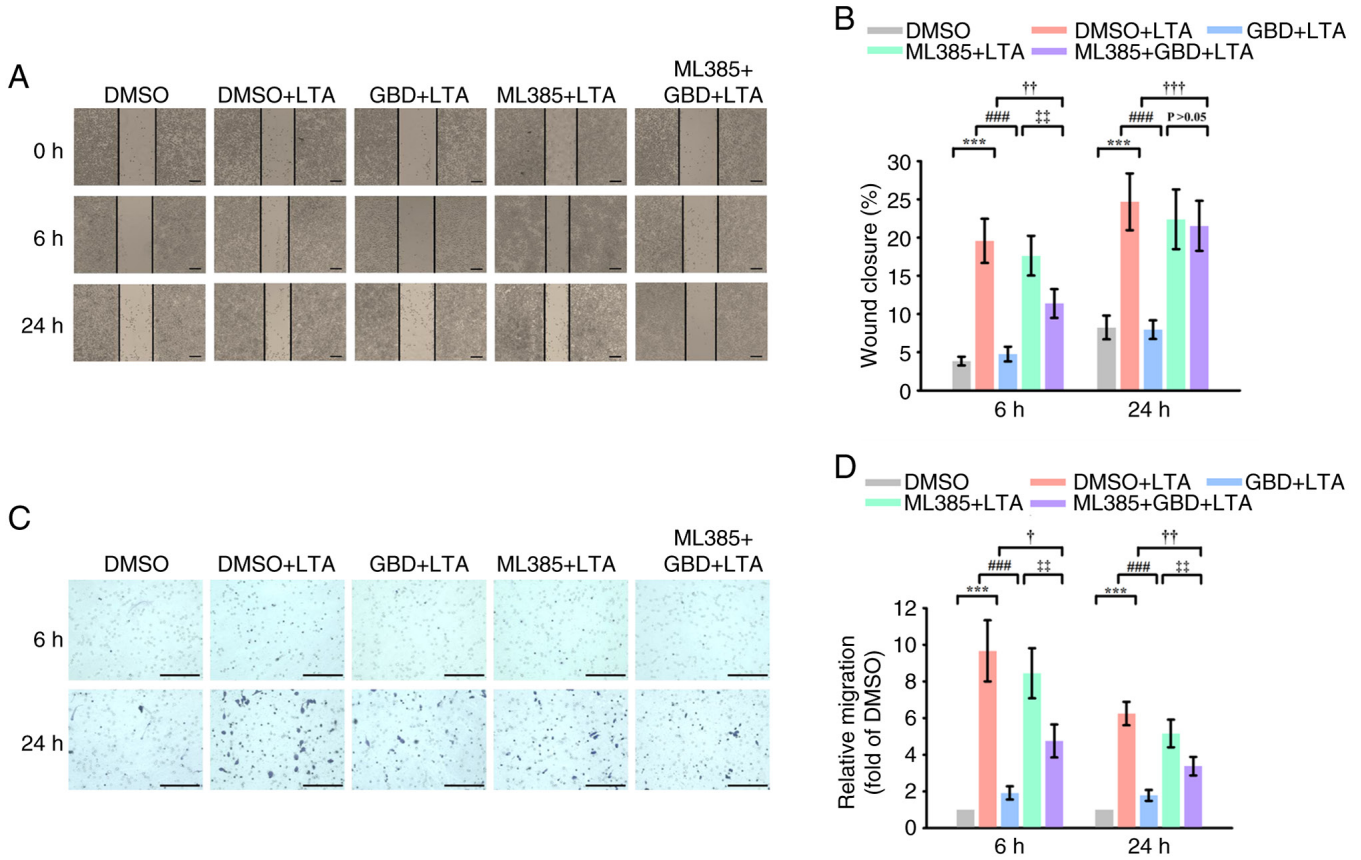

Figure 6. GBD inhibits LTA-induced macrophage migration through Nrf2 activation. MH-S cells were pretreated with the indicated compounds for 30 min and then stimulated with LTA. (A) Representative wound healing images 0, 6, and 24 h after LTA stimulation. (B) Quantification of wound closure. (C) Representative images of Transwell migration at 6 h and 24 h after LTA stimulation. Migrated cells on the lower surface of the membrane were fixed, stained with crystal violet and images captured under an inverted light microscope. Scale bar, 200 μm. (D) Quantification of migrated cells. Data are presented as means ± SD. ***P<0.001 vs. DMSO; $^{###}$P<0.001 vs. DMSO+LTA; †P<0.05, ††P<0.01 and †††P<0.001 vs. GBD+LTA; ‡‡P<0.01 vs. ML385+LTA. GBD, glabridin; LTA, lipoteichoic acid; Nrf2, nuclear factor erythroid 2-related factor 2; DMSO, dimethyl sulfoxide.

novel avenue for therapies targeting macrophage dynamics in inflammation-related conditions.

Notably, lipopolysaccharide (LPS), which is derived from Gram-negative bacteria, primarily activates TLR4 signaling. Although both LTA and LPS initiate innate immune responses, their receptor engagement, downstream signaling profiles and temporal dynamics differ. Clinically, LPS-related endotoxemia is commonly associated with sepsis caused by Gram-negative infections, such as *Escherichia coli* or *Pseudomonas aeruginosa*. By contrast, LTA is implicated in Gram-positive bacterial infections, including *Staphylococcus aureus*, *Streptococcus pneumoniae*, and *Enterococcus species*, which contribute to pneumonia, endocarditis, and skin and soft tissue infections (24). In research on pulmonary diseases, both LPS and LTA have been employed as experimental stimuli to mimic bacterial infection and elicit innate immune responses in lung models. In animal studies, LPS is widely used to induce acute lung injury or acute respiratory distress syndrome (ARDS) because of its potent ability to activate neutrophils, disrupt endothelial barriers, and promote cytokine storms through TLR4-dependent signaling (25,26). By contrast, LTA activates alveolar macrophages, modulates surfactant expression, and contributes to the development of Gram-positive pneumonia (27). Although LTA-induced responses are generally less systemically severe than LPS-induced responses are, evidence increasingly suggests that chronic or repeated exposure to LTA can provoke sustained lung inflammation, epithelial damage, and macrophage-driven remodeling (27,28). These differential effects underscore a need to distinguish between Gram-negative and Gram-positive bacterial stimuli in evaluations of pulmonary immune responses and corresponding therapeutic strategies. In the present study, LTA stimulation induced a marked increase in alveolar macrophage migration, elevated ROS levels and activated the Nrf2/HO-1 pathway. These findings indicated that Gram-positive bacterial components influence macrophage behavior through stress-responsive mechanisms, providing novel insights into cell dynamics during bacterial exposure.

Alveolar macrophages are specialized tissue-resident immune cells located within the alveolar lumen, where they play a critical role in maintaining pulmonary homeostasis and coordinating immune surveillance (29). Unlike circulating monocytes or recruited inflammatory macrophages, alveolar macrophages originate from fetal monocytes and their population is self-renewing (30,31). Under steady-state conditions, they exhibit a relatively quiescent phenotype, clearing inhaled particles, apoptotic cells and pathogens without eliciting excessive inflammation (32). Due to their position at the interface between the airway epithelium and the external environment, their activity must be tightly regulated to avoid compromising

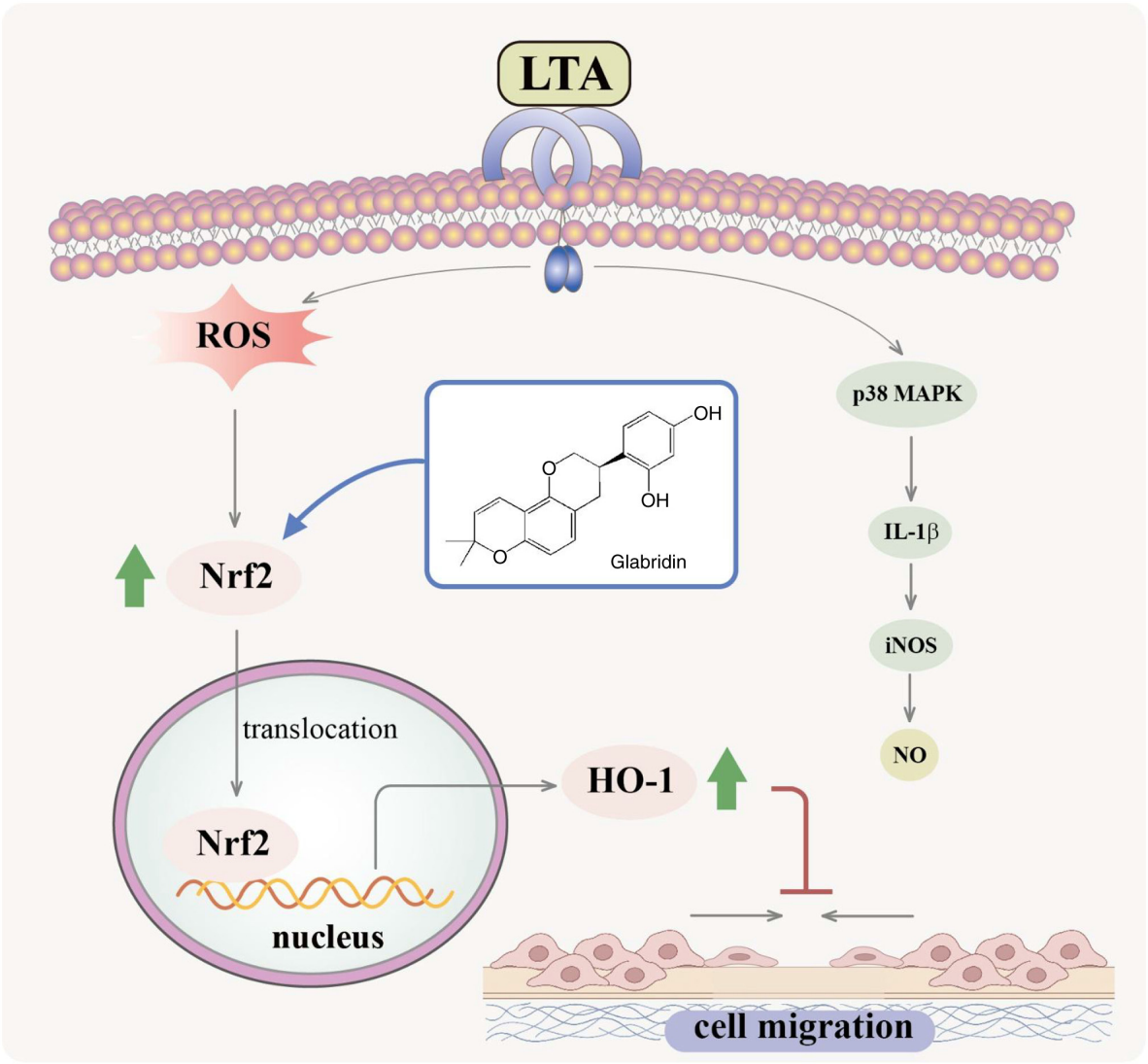

Figure 7. Schematic of GBD-induced modulation of macrophage migration *in vitro*. Upon LTA stimulation, MH-S cells increase ROS production, activating Nrf2 and upregulating HO-1. GBD thus modulateS cell migration by increasing Nrf2 nuclear translocation and HO-1 expression. GBD, glabridin; LTA, lipoteichoic acid; ROS, reactive oxygen species; Nrf2, nuclear factor erythroid 2-related factor 2; HO-1, heme oxygenase-1.

alveolar barrier integrity (33). In the present study, MH-S cells were employed as an *in vitro* model because of their established relevance in studies of pulmonary innate immunity (34). This model provided a suitable framework to investigate the regulatory effects of GBD on alveolar macrophage migration.

The Nrf2/HO-1 pathway is a central regulator of cellular homeostasis under stress (35-37). Upon activation, the transcription factor Nrf2 translocates to the nucleus to induce cytoprotective genes (38). HO-1 was chosen as the canonical marker because it is not only a robustly induced Nrf2 target in macrophages (39), but also because its enzymatic products actively regulate inflammation and macrophage migration (40,41), positioning it at the mechanistic nexus of GBD's effects. While this pathway is known to modulate immune cell behavior, including migration (42,43), its role in response to specific bacterial components such as LTA was unclear.

To further refine the mechanistic profile, the present study also examined additional inflammatory and oxidative stress markers. GBD displayed a selective pattern of activity. GBD markedly suppressed LTA-induced IL-1β mRNA expression, yet had no effect on TNF-α or IL-6 levels. Similarly, while the steady-state antioxidant enzyme SOD1 remained unchanged, GBD markedly reduced later-stage oxidative markers, including 24-h lipid peroxidation (MDA) and nitric oxide (NO) production. These supplementary findings suggested that HO-1 is likely to be a prominent downstream effector of GBD in this setting, consistent with reports that the Nrf2/HO-1 axis can provide real-time protection against oxidative insults (37,38). and that HO-1 products can modulate inflammatory cell migration (44,45).

Dysregulated macrophage migration has been implicated in inflammatory lung diseases, contributing to both excessive inflammation and impaired pathogen clearance (46). While alveolar macrophages are generally sessile under homeostatic conditions (4), they can adopt a migratory phenotype upon microbial stimulation to support immune surveillance (33,47). To assess GBD's effect on this process, the present study employed two complementary approaches: The wound-healing assay a well-established method for assessing collective

motility and the Transwell assay for directional chemotaxis. In both systems, LTA stimulation increased macrophage migration, whereas GBD treatment reduced this response. The inhibitory effect was attenuated by the Nrf2 inhibitor ML385, suggesting that Nrf2 signaling contributes to this regulation. Consistent outcomes from both assays supported the reliability of these findings and provided a rationale for further validation of the underlying mechanism.

To rigorously validate the essential role of Nrf2, the present study employed both pharmacological inhibition and genetic knockdown approaches. The Nrf2 inhibitor ML385 partly reversed the anti-migratory effects of GBD, while silencing Nrf2 with siRNA markedly attenuated the GBD-induced upregulation of HO-1 mRNA. This convergence of evidence from two distinct methodologies supported the involvement of Nrf2/HO-1 signaling in mediating the effect of GBD. Furthermore, the specific downstream effectors mediating this anti-migratory response remain to be elucidated. Future studies should therefore examine additional Nrf2 targets, including other cytoprotective enzymes beyond HO-1, such as NQO1, as well as proteins directly involved in cell motility, particularly matrix metalloproteinases (such as MMP-2 and MMP-9), which are functionally linked to macrophage migration (48).

The present study offered novel mechanistic insights regarding how GBD affects macrophage behavior under LTA stimulation. LTA exposure was sufficient to induce pronounced migratory activity in alveolar macrophages, highlighting its capacity to modulate innate immune cell motility. GBD pretreatment markedly reduced macrophage migration, possibly because of the increased nuclear accumulation of Nrf2 and elevated HO-1 expression. Pharmacological inhibition with ML385 and genetic knockdown with siRNA both attenuated the antimigratory effects of GBD, supporting the involvement of Nrf2 activation in mediating this response. To the best of our knowledge, this is the first study to demonstrate that GBD modulated LTA-induced alveolar macrophage migration through mechanisms involving the Nrf2/HO-1 pathway. These findings revealed a novel functional aspect of GBD in controlling macrophage dynamics, suggesting it holds potential relevance in preventing dysregulated cell migration associated with pulmonary inflammation.

The clinical implications of modulating macrophage migration are extensive. Aberrant cell motility is a recognized pathological feature in a wide range of diseases; for instance, excessive macrophage infiltration drives pulmonary conditions such as COPD and ARDS, while insufficient migration can impair pathogen clearance and tissue repair (46,49-52). Beyond the lung, macrophage trafficking is also pivotal in the progression of cancer, atherosclerosis and autoimmune diseases (53). The present study thus positioned GBD as a potential modulator in these contexts. Notably, the temporal dynamics of GBD's antimigratory effects have important therapeutic implications. The rapid onset of action suggested potential utility in acute inflammatory conditions where early intervention is critical. However, the attenuated long-term effects indicated that sustained therapeutic benefits may require optimized dosing regimens or combination approaches. This nuanced profile supported the strategy of using pharmacological agents to modulate, rather than abolish, macrophage migration to restore immune balance. Therefore, GBD may hold potential as a modulator for diseases involving immune cell dysregulation.

Macrophage migration and polarization are functionally interlinked, particularly under inflammatory conditions where M1-polarized cells exhibit enhanced motility (54-56). This relationship is often bidirectional, as migration into a pro-inflammatory microenvironment can further reinforce M1 polarization (57). In this context, the LTA-induced migration observed may reflect a shift toward an activated, pro-inflammatory M1-like state. Measurement of nitric oxide (NO) production, a marker often associated with M1 activation, supported this notion. However, a more comprehensive assessment using canonical polarization markers (such as iNOS, CD86 and Arg1) will be valuable in future studies to further establish this link.

While the present study established a mechanistic link between GBD, Nrf2/HO-1 activation and suppressed macrophage migration, several limitations should be acknowledged. One limitation is that the investigation was confined to *in vitro* models. Future *in vivo* studies are necessary to validate the physiological relevance of the findings and to assess downstream pathophysiological implications, such as the effect of GBD on alveolar-capillary barrier integrity. Another limitation is that the mechanistic focus was restricted to the Nrf2/HO-1 axis. The role of other critical components of cell motility, particularly adhesion molecules (such as integrins, selectins), was not assessed and represents an important avenue for future research. A further limitation is that the analysis of oxidative stress was not exhaustive. Future work should therefore include a more comprehensive profiling of oxidative stress parameters; for instance, by measuring protein carbonyl formation and assessing the cellular glutathione antioxidant system. Finally, for GBD to advance as a pharmacologically viable compound, its pharmacokinetic profile, particularly bioavailability and metabolic stability, will require comprehensive evaluation (58). The observed time-dependent attenuation of GBD's effects in the present study also highlighted the need to investigate optimal dosing regimens for sustained therapeutic efficacy.

The present study demonstrated that GBD attenuated LTA-induced alveolar macrophage migration by activating the Nrf2/HO-1 signaling pathway. It integrated molecular, cellular and functional analyses to reveal a regulatory mechanism by which GBD affected macrophage motility in response to bacterial stimulation. These findings broadened the current understanding of the biological effects of GBD and suggested its potential as a modulatory agent of immune cell behavior in disease contexts. Future *in vivo* investigations and pharmacological profiling are required to further validate the therapeutic utility and translational applicability of GBD to inform the development of novel therapeutic strategies for inflammatory lung diseases.

Acknowledgements

Not applicable.

Funding

The present study was supported by the National Science and Technology Council, Taiwan, R.O.C.

(grant nos. NSTC 112-2320-B-038-037-MY3 and NSTC 113-2320-B341-002-MY3), Shin Kong Wu Ho-Su Memorial Hospital (grant no. 2025SKHAND011) and Chi Mei Medical Center-Taipei Medical University (grant no. 111CM-TMU-07).

Availability of data and materials

The data generated in the present study are included in the figures and/or tables of this article.

Authors' contributions

JRS designed the study. CHH and CMY wrote the manuscript. CHH, CMY, CCC, TLY, AGD and CCH performed the experiments. CCC, TLY and AGD analyzed the data. CMY and JRS confirm the authenticity of all the raw data. All authors have read and approved the final manuscript.

Ethical approval and consent to participate

Not applicable.

Patient consent for publication

Not applicable.

Competing interests

The authors declare that they have no competing interests.

References

1. Takeuchi O, Hoshino K, Kawai T, Sanjo H, Takada H, Ogawa T, Takeda K and Akira S: Differential roles of TLR2 and TLR4 in recognition of gram-negative and gram-positive bacterial cell wall components. Immunity 11: 443-451, 1999.
2. Pai AB, Patel H, Prokopienko AJ, Alsaffar H, Gertzberg N, Neumann P, Punjabi A and Johnson A: Lipoteichoic acid from staphylococcus aureus induces lung endothelial cell barrier dysfunction: Role of reactive oxygen and nitrogen species. PLoS One 7: e49209, 2012.
3. Percy MG and Gründling A: Lipoteichoic acid synthesis and function in gram-positive bacteria. Annu Rev Microbiol 68: 81-100, 2014.
4. Hussell T and Bell TJ: Alveolar macrophages: Plasticity in a tissue-specific context. Nat Rev Immunol 14: 81-93, 2014.
5. Boyd AR, Shivshankar P, Jiang S, Berton MT and Orihuela CJ: Age-related defects in TLR2 signaling diminish the cytokine response by alveolar macrophages during murine pneumococcal pneumonia. Exp Gerontol 47: 507-518, 2012.
6. Liu CF, Drocourt D, Puzo G, Wang JY and Riviere M: Innate immune response of alveolar macrophage to house dust mite allergen is mediated through TLR2/-4 co-activation. PLoS One 8: e75983, 2013.
7. Aggarwal S, Dimitropoulou C, Lu Q, Black SM and Sharma S: Glutathione supplementation attenuates lipopolysaccharide-induced mitochondrial dysfunction and apoptosis in a mouse model of acute lung injury. Front Physiol 3: 161, 2012.
8. Birben E, Sahiner UM, Sackesen C, Erzurum S and Kalayci O: Oxidative stress and antioxidant defense. World Allergy Organ J 5: 9-19, 2012.
9. Malainou C, Abdin SM, Lachmann N, Matt U and Herold S: Alveolar macrophages in tissue homeostasis, inflammation, and infection: Evolving concepts of therapeutic targeting. J Clin Invest 133: e170501, 2023.
10. Harvey CJ, Thimmulappa RK, Sethi S, Kong X, Yarmus L, Brown RH, Feller-Kopman D, Wise R and Biswal S: Targeting Nrf2 signaling improves bacterial clearance by alveolar macrophages in patients with COPD and in a mouse model. Sci Transl Med 3: 78ra32, 2011.
11. Itoh K, Chiba T, Takahashi S, Ishii T, Igarashi K, Katoh Y, Oyake T, Hayashi N, Satoh K, Hatayama I, *et al*: An Nrf2/small Maf heterodimer mediates the induction of phase II detoxifying enzyme genes through antioxidant response elements. Biochem Biophys Res Commun 236: 313-322, 1997.
12. Ma Q: Role of nrf2 in oxidative stress and toxicity. Annu Rev Pharmacol Toxicol 53: 401-426, 2013.
13. Itoh K, Wakabayashi N, Katoh Y, Ishii T, Igarashi K, Engel JD and Yamamoto M: Keap1 represses nuclear activation of antioxidant responsive elements by Nrf2 through binding to the amino-terminal Neh2 domain. Genes Dev 13: 76-86, 1999.
14. Ryter SW, Alam J and Choi AM: Heme oxygenase-1/carbon monoxide: From basic science to therapeutic applications. Physiol Rev 86: 583-650, 2006.
15. Meng X, Hu L and Li W: Baicalin ameliorates lipopolysaccharide-induced acute lung injury in mice by suppressing oxidative stress and inflammation via the activation of the Nrf2-mediated HO-1 signaling pathway. Naunyn Schmiedebergs Arch Pharmacol 392: 1421-1433, 2019.
16. Luan R, Ding D and Yang J: The protective effect of natural medicines against excessive inflammation and oxidative stress in acute lung injury by regulating the Nrf2 signaling pathway. Front Pharmacol 13: 1039022, 2022.
17. Shin J, Choi LS, Jeon HJ, Lee HM, Kim SH, Kim KW, Ko W, Oh H and Park HS: Synthetic glabridin derivatives inhibit LPS-induced inflammation via MAPKs and NF-κB Pathways in RAW264.7 macrophages. Molecules 28: 2135, 2023.
18. Shu L, Zhang Z, Wang N, Yin Q, Chao Y and Ge X: Glabridin ameliorates hemorrhagic shock induced acute kidney injury by activating Nrf2/HO-1 pathway. Biochim Biophys Acta Mol Basis Dis 1871: 167810, 2025.
19. Livak KJ and Schmittgen TD: Analysis of relative gene expression data using real-time quantitative PCR and the 2(-Delta Delta C(T)) method. Methods 25: 402-408, 2001.
20. Murrey MW, Ng IT and Pixley FJ: The role of macrophage migratory behavior in development, homeostasis and tumor invasion. Front Immunol 15: 1480084, 2024.
21. Rodriguez-Morales P and Franklin RA: Macrophage phenotypes and functions: Resolving inflammation and restoring homeostasis. Trends Immunol 44: 986-998, 2023.
22. Tran N and Mills EL: Redox regulation of macrophages. Redox Biol 72: 103123, 2024.
23. Breßer M, Siemens KD, Schneider L, Lunnebach JE, Leven P, Glowka TR, Oberländer K, De Domenico E, Schultze JL, Schmidt J, *et al*: Macrophage-induced enteric neurodegeneration leads to motility impairment during gut inflammation. EMBO Mol Med 17: 301-335, 2025.
24. Gatica S, Fuentes B, Rivera-Asin E, Ramírez-Céspedes P, Sepúlveda-Alfaro J, Catalán EA, Bueno SM, Kalergis AM, Simon F, Riedel CA and Melo-Gonzalez F: Novel evidence on sepsis-inducing pathogens: From laboratory to bedside. Front Microbiol 14: 1198200, 2023.
25. He J, Zhao Y, Fu Z, Chen L, Hu K, Lin X, Wang N, Huang W, Xu Q, He S, *et al*: A novel tree shrew model of lipopolysaccharide-induced acute respiratory distress syndrome. J Adv Res 56: 157-165, 2024.
26. Zhang Y, Han Z, Jiang A, Wu D, Li S, Liu Z, Wei Z, Yang Z and Guo C: Protective effects of pterostilbene on lipopolysaccharide-induced acute lung injury in mice by inhibiting NF-κB and activating Nrf2/HO-1 signaling pathways. Front Pharmacol 11: 591836, 2021.
27. Knapp S, von Aulock S, Leendertse M, Haslinger I, Draing C, Golenbock DT and van der Poll T: Lipoteichoic acid-induced lung inflammation depends on TLR2 and the concerted action of TLR4 and the platelet-activating factor receptor. J Immunol 180: 3478-3484, 2008.
28. Hoogerwerf JJ, de Vos AF, Bresser P, van der Zee JS, Pater JM, de Boer A, Tanck M, Lundell DL, Her-Jenh C, Draing C, *et al*: Lung inflammation induced by lipoteichoic acid or lipopolysaccharide in humans. Am J Respir Crit Care Med 178: 34-41, 2008.
29. Hou F, Xiao K, Tang L and Xie L: Diversity of macrophages in lung homeostasis and diseases. Front Immunol 12: 753940, 2021.
30. Guilliams M, De Kleer I, Henri S, Post S, Vanhoutte L, De Prijck S, Deswarte K, Malissen B, Hammad H and Lambrecht BN: Alveolar macrophages develop from fetal monocytes that differentiate into long-lived cells in the first week of life via GM-CSF. J Exp Med 210: 1977-1992, 2013.
31. Röszer T: Understanding the biology of self-renewing macrophages. Cells 7: 103, 2018.

32. Guan F, Wang R, Yi Z, Luo P, Liu W, Xie Y, Liu Z, Xia Z, Zhang H and Cheng Q: Tissue macrophages: Origin, heterogenity, biological functions, diseases and therapeutic targets. Signal Transduct Target Ther 10: 93, 2025.
33. Ahmad S, Nasser W and Ahmad A: Epigenetic mechanisms of alveolar macrophage activation in chemical-induced acute lung injury. Front Immunol 15: 1488913, 2024.
34. Mbawuike IN and Herscowitz HB: MH-S, a murine alveolar macrophage cell line: Morphological, cytochemical, and functional characteristics. J Leukoc Biol 46: 119-127, 1989.
35. Loboda A, Damulewicz M, Pyza E, Jozkowicz A and Dulak J: Role of Nrf2/HO-1 system in development, oxidative stress response and diseases: An evolutionarily conserved mechanism. Cell Mol Life Sci 73: 3221-3247, 2016.
36. Li N, Hao L, Li S, Deng J, Yu F, Zhang J, Nie A and Hu X: The NRF-2/HO-1 signaling pathway: A promising therapeutic target for metabolic dysfunction-associated steatotic liver disease. J Inflamm Res 17: 8061-8083, 2024.
37. Su H, Wang Z, Zhou L, Liu D and Zhang N: Regulation of the Nrf2/HO-1 axis by mesenchymal stem cells-derived extracellular vesicles: Implications for disease treatment. Front Cell Dev Biol 12: 1397954, 2024.
38. O'Rourke SA, Shanley LC and Dunne A: The Nrf2-HO-1 system and inflammaging. Front Immunol 15: 1457010, 2024.
39. Alam J and Cook JL: How many transcription factors does it take to turn on the heme oxygenase-1 gene? Am J Respir Cell Mol Biol 36: 166-174, 2007.
40. Vijayan V, Wagener FADTG and Immenschuh S: The macrophage heme-heme oxygenase-1 system and its role in inflammation. Biochem Pharmacol 153: 159-167, 2018.
41. Wang L and He C: Nrf2-mediated anti-inflammatory polarization of macrophages as therapeutic targets for osteoarthritis. Front Immunol 13: 967193, 2022.
42. Feng R, Morine Y, Ikemoto T, Imura S, Iwahashi S, Saito Y and Shimada M: Nrf2 activation drive macrophages polarization and cancer cell epithelial-mesenchymal transition during interaction. Cell Commun Signal 16: 54, 2018.
43. Han H, Gao Y, Chen B, Xu H, Shi C, Wang X, Liang Y, Wu Z, Wang Z, Bai Y and Wu C: Nrf2 inhibits M1 macrophage polarization to ameliorate renal ischemia-reperfusion injury through antagonizing NF-κB signaling. Int Immunopharmacol 143: 113310, 2024.
44. Jagadeesh ASV, Fang X, Kim SH, Guillen-Quispe YN, Zheng J, Surh YJ and Kim SJ: Non-canonical vs. canonical functions of heme oxygenase-1 in cancer. J Cancer Prev 27: 7-15, 2022.
45. Freitas A, Alves-Filho JC, Secco DD, Neto AF, Ferreira SH, Barja-Fidalgo C and Cunha FQ: Heme oxygenase/carbon monoxide-biliverdin pathway down regulates neutrophil rolling, adhesion and migration in acute inflammation. Br J Pharmacol 149: 345-354, 2006.
46. Cheng P, Li S and Chen H: Macrophages in lung injury, repair, and fibrosis. Cells 10: 436, 2021.
47. Chen S, Saeed AFUH, Liu Q, Jiang Q, Xu H, Xiao GG, Rao L and Duo Y: Macrophages in immunoregulation and therapeutics. Signal Transduct Target Ther 8: 207, 2023.
48. Ngo V and Duennwald ML: Nrf2 and oxidative stress: A general overview of mechanisms and implications in human disease. Antioxidants (Basel) 11: 2345, 2022.
49. Matthay MA and Zemans RL: The acute respiratory distress syndrome: Pathogenesis and treatment. Annu Rev Pathol 6: 147-163, 2011.
50. Barnes PJ: Inflammatory mechanisms in patients with chronic obstructive pulmonary disease. J Allergy Clin Immunol 138: 16-27, 2016.
51. Gordon S and Plüddemann A: Macrophage clearance of apoptotic cells: A critical assessment. Front Immunol 9: 127, 2018.
52. Wynn TA and Vannella KM: Macrophages in tissue repair, regeneration, and fibrosis. Immunity 44: 450-462, 2016.
53. Gordon S, Plüddemann A and Martinez Estrada F: Macrophage heterogeneity in tissues: Phenotypic diversity and functions. Immunol Rev 262: 36-55, 2014.
54. Mantovani A, Biswas SK, Galdiero MR, Sica A and Locati M: Macrophage plasticity and polarization in tissue repair and remodelling. J Pathol 229: 176-185, 2013.
55. Murray PJ, Allen JE, Biswas SK, Fisher EA, Gilroy DW, Goerdt S, Gordon S, Hamilton JA, Ivashkiv LB, Lawrence T, *et al*: Macrophage activation and polarization: Nomenclature and experimental guidelines. Immunity 41: 14-20, 2014.
56. Auffray C, Fogg D, Garfa M, Elain G, Join-Lambert O, Kayal S, Sarnacki S, Cumano A, Lauvau G and Geissmann F: Monitoring of blood vessels and tissues by a population of monocytes with patrolling behavior. Science 317: 666-670, 2007.
57. Lawrence T and Natoli G: Transcriptional regulation of macrophage polarization: Enabling diversity with identity. Nat Rev Immunol 11: 750-761, 2011.
58. Xie L, Diao Z, Xia J, Zhang J, Xu Y, Wu Y, Liu Z, Jiang C, Peng Y, Song Z, *et al*: Comprehensive evaluation of metabolism and the contribution of the hepatic first-pass effect in the bioavailability of glabridin in rats. J Agric Food Chem 71: 1944-1956, 2023.